JOC Article

Conformational Analysis of Sulfur-Containing 6-Deoxy-L-hexose Derivatives by Molecular Modeling and NMR Spectroscopy. A Theoretical Study and Experimental Evidence of Intramolecular Nonbonded Interactions between Sulfur and Oxygen

Mabel Fragoso-Serrano,[†,‡] Georgina Guillén-Jaramillo,[‡] Rogelio Pereda-Miranda,*[,‡] and Carlos M. Cerda-García-Rojas*[,†]

Departamento de Química, Centro de Investigación y de Estudios Avanzados del Instituto Politécnico Nacional, Apartado 14-740, Mexico City 07000, Mexico, and Departamento de Farmacia, Facultad de Química, Universidad Nacional Autónoma de México, Ciudad Universitaria, Mexico City 04510, Mexico

pereda@servidor.unam.mx; ccerda@mail.cinvestav.mx

Received April 16, 2003

6-Deoxy-L-mannose diphenyldithioacetal (**1**) unexpectedly gave the rearranged products phenyl 3,4-di-*O*-acetyl-2-*S*-phenyl-1,2-dithio-6-deoxy-*β*-L-glucopyranoside (**9**) and 3,4-di-*O*-acetyl-2,5-anhydro-6-deoxy-L-glucose diphenyldithioacetal (**10**) upon treatment with acetyl chloride, while 6-deoxy-L-mannose ethylenedithioacetal (**3**) yielded (4a*R*,6*S*,7*S*,8*R*,8a*S*)-7,8-diacetyloxy-6-methylhexahydro-4a*H*-[1,4]dithiino[2,3b]pyran (**11**), whose structure was further confirmed by X-ray diffraction, and 3,4-di-*O*-acetyl-2,5-anhydro-L-rhamnose ethylenedithioacetal (**12**). The geometry of the four rearranged products as well as that of 1-thio-6-deoxy-L-mannopyranosides **5** and **7** and their acetyl derivatives **6** and **8** was studied by density functional theory (B3LYP/6-31G*) molecular models, in combination with a Karplus-type analysis of the NMR vicinal coupling constants, revealing that the six-membered ring of pyranosides **5**−**9** and **11** exists in a slightly distorted chair conformation (6−13% distortion) and that the conformational behavior of the 2,5-anhydro-6-deoxy-L-glucose dithioacetals **10** and **12** is strongly influenced by the presence of stabilizing intramolecular nonbonded sulfur−oxygen 1,4- and 1,5-interactions. Compounds **9**−**12** were formed by a molecular rearrangement via sulfonium ion intermediates followed by stereoselective intramolecular cyclizations as formulated by the quantum chemical calculations performed in the present study.

Introduction

Sulfur-containing monosaccharide derivatives provide simple representative models to explore a wide variety of conformational aspects also present in relevant complex biomolecules.[1−3] An interesting example of the latter are the thiooligosaccharides which have been synthesized[4] as tools for studies in structural biology for they represent the largest class of competitive inhibitors of glycoside hydrolases.[5,6] Part of our ongoing research program is directed toward the application of molecular modeling in the total stereochemical elucidation of cytotoxic 6-tetraacetyloxyheptenyl-5,6-dihydro-α-pyrones.[7] We have been preparing some polyoxygenated molecules derived from 6-deoxy-L-hexoses, such as dithioacetals, which are then generally synthesized as versatile chiral building blocks,[8] to provide us with an adequate group of compounds to investigate the intramolecular sulfur−oxygen interactions by quantum mechanical and NMR spectroscopy studies. This approach, which is comparable to classical NMR experimental studies (e.g., variable-temperature measurements), proved to be an effective methodology for determining the conformational equilibria of monosaccharides[9] and heterocyclic systems.[10]

For the present investigation, we used density functional theory (DFT)[11] calculations in conjunction with

* To whom correspondence should be addressed. Phone: +52-55-5061-3800 ext. 4035 (C.M.C.-G.-R.). Fax: +52-55-5747-7137 (C.M.C.-G.-R.); +52-55-5622-5288 (R.P.-M.).

† Centro de Investigación y de Estudios Avanzados del Instituto Politécnico Nacional.

‡ Universidad Nacional Autónoma de México.

(1) Driguez, H. *Chembiochem* **2001**, *2*, 311−318.

(2) Cohen, S. B.; Halcomb, R. L. *J. Org. Chem.* **2000**, *65*, 6145−6152.

(3) Ding, Y.; Contour-Galcera, M.-O.; Ebel, J.; Ortiz-Mellet, C.; Defaye, J. *Eur. J. Org. Chem.* **1999**, 1143−1152.

(4) (a) Ibatullin, F. M.; Shabalin, K. A.; Jänis, J. V.; Selivanov, S. I. *Tetrahedron Lett.* **2001**, *42*, 4565−4567. (b) Josse, S.; Le Gal, J.; Pipelier, M.; Cléophax, J.; Olesker, A.; Pradère, J.-P.; Dubreuil, D. *Tetrahedron Lett.* **2002**, *43*, 237−239.

(5) Svansson, L.; Johnston, D. B.; Gu, J. H.; Patrick, B.; Pinto, B. M. *J. Am. Chem. Soc.* **2000**, *122*, 10769−10775.

(6) Ghavami, A.; Johnston, B. D.; Jensen, M. T.; Svensson, B.; Pinto, B. M. *J. Am. Chem. Soc.* **2001**, *123*, 6268−6271.

(7) Pereda-Miranda, R.; Fragoso-Serrano, M.; Cerda-García-Rojas, C. M. *Tetrahedron* **2001**, *57*, 43−57.

(8) Lichtenthaler, W. F. Enantiopure Building Blocks from Sugars and their Utilization in Natural Product Synthesis. In *Modern Synthetic Methods*; Scheffold, R., Ed.; VCH: Weinheim, Germany/New York, 1992; Vol. 6, pp 273−376.

(9) (a) Hricovíni, M.; Tvaroška, I.; Hirsch, J. *Carbohydr. Res.* **1990**, *198*, 193−203. (b) Tvaroška, I.; Mazeau, K.; Blanc-Muesser, M.; Lavaitte, S.; Driguez, H.; Taravel, F. R. *Carbohydr. Res.* **1992**, *229*, 225−231. (c) Tvaroška, I.; Taravel, F. R.; Utille, J. P.; Carver, J. P. *Carbohydr. Res.* **2002**, *337*, 353−367.

(10) Tähtinen, P.; Bagno A.; Klika, K. D.; Pihlaja, K. *J. Am. Chem. Soc.* **2003**, *125*, 4609−4618.

10.1021/jo034492k CCC: $25.00
Published on Web 08/20/2003

NMR data to explore the conformational behavior of a series of 2,5-anhydro-6-deoxy-L-glucose dithioacetals. The relevant influence of 1,4- and 1,5-interactions in the conformational equilibria of these compounds is also discussed. A limited number of investigations have been focused on the energetics associated with this type of interaction between nonbonded sulfur and oxygen atoms. These geometry optimizations,[12] in conjunction with X-ray diffraction determined molecular structures,[13] allowed for the calculation of the S−O distances, which ranged from 2.7 to 3.1 Å.

The new cyclic substances were unexpectedly obtained from the preparation of peracetylated dithioacetals of 6-deoxy-L-mannose for which we used benzenethiol in aqueous trifluoroacetic acid[14] followed by treatments with acetyl chloride. These new products were formed by molecular rearrangements via sulfonium ion intermediates followed by stereoselective intramolecular cyclizations.[15,16] A reaction mechanism for the formation of these new sulfur-containing cyclic derivatives was outlined according to quantum chemical calculations.

Results and Discussion

Preparation and Structure Elucidation of Sulfur-Containing Derivatives. 6-Deoxy-L-mannose diphenyldithioacetal (**1**) (Chart 1) was obtained using the reaction conditions described by Funabashi et al.,[14] through treatment of 6-deoxy-L-mannose (L-rhamnose) with benzenethiol in 90% aqueous trifluoroacetic acid. This reaction produced the expected product **1** as well as good yields of phenyl 1-thio-6-deoxy-L-mannopyranosides **5** and **7**, all subsequently easily purified by HPLC. Treatment of both cyclic substances with acetyl chloride yielded **6** and **8**, respectively. Compounds **5**, **6**, and **8** are extensively employed in the synthesis of relevant bioactive compounds,[17−19] whereas phenyl 1-thio-6-deoxy-β-L-mannopyranoside (**7**) is described herein for the first time. The structure and stereochemistry of **7** were easily deduced by comparison of its ^{1}H and ^{13}C NMR signals with those of the methyl 1-thio-6-deoxy-L-mannopyranosides[17] and triacetyl derivative **8**. Treatment of **1** with acetyl chloride afforded the expected product **2** together with important amounts of the new phenyl 3,4-di-*O*-acetyl-2-*S*-phenyl-1,2-dithio-6-deoxy-β-L-glucopyranoside (**9**) and 3,4-di-*O*-acetyl-2,5-anhydro-6-deoxy-L-glucose

CHART 1

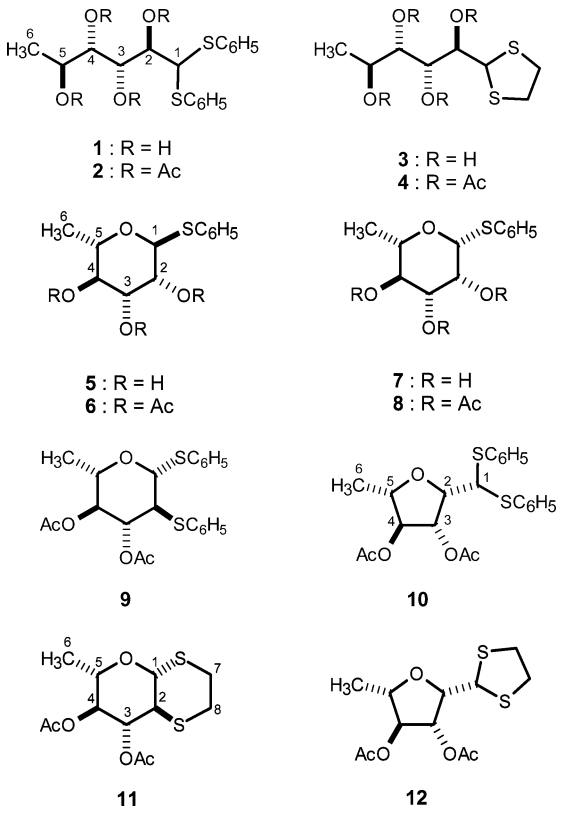

diphenyldithioacetal (**10**). Subjecting ethylenedithioacetal **3** to a similar treatment[7] produced compound **4** and the new cyclic derivatives (4a*R*,6*S*,7*S*,8*R*,8a*S*)-7,8-diacetyloxy-6-methylhexahydro-4a*H*-[1,4]dithiino[2,3*b*]pyran (**11**) and 3,4-di-*O*-acetyl-2,5-anhydro-L-rhamnose ethylenedithioacetal (**12**) along with trace amounts of compound **19**. The structure for the last mentioned compound is included in the reaction mechanism depicted in Scheme 1. The structures for all these new products were determined by 1D and 2D spectroscopy, including COSY, HMQC, and HMBC experiments. The stereochemistry for the chiral center C2 on **9** and **11** was assigned on the basis of the observed NOESY correlations (H2−H4, H1−H5, H1−H3, and H3−H5) although both coupling constants ($J_{1,2} = J_{2,3} = 9-11$ Hz) for its corresponding methine signal provided enough evidence for the equatorial orientation of the thiophenyl substituent. The same information was obtained from the observed NOE between H2 and H5 and used to confirm the cis relationship for the substituents at C2 and C5 in the tetrahydrofurane ring in **10** and **12**. X-ray diffraction analysis of compound **11** was used to verify its structure and stereochemistry (Figure 1).

Conformational Analysis by Molecular Modeling and NMR Spectroscopy. Using a Dreiding model guided systematic conformational search, the structures for pyranoside derivatives **5**−**9** and **11**, as well as those for the 2,5-anhydrohexose derivatives **10** and **12**, were initially analyzed by molecular mechanics employing the MMFF94 force field.[20] Their minimum energy conformers were generated after taking into consideration the following assumptions: (a) that the number of possible conformers could be established and limited by varying each of the endocyclic torsion angles in steps of 30° within

(11) (a) Perdew, J. P. *Phys. Rev. B* **1986**, *33*, 8822−8824. (b) Becke, A. D. *Phys. Rev. A* **1988**, *38*, 3098−3100.
(12) (a) Burling, F. T.; Goldstein, B. M. *J. Am. Chem. Soc.* **1992**, *114*, 2313−2320. (b) Markham, G. D.; Bock, C. W. *J. Mol. Struct.: THEOCHEM* **1997**, *418*, 139−154. (c) Markham, G. D.; Bock, C. L.; Trachtman, M.; Bock, C. W. *Struct. Chem.* **1999**, *10*, 263−276.
(13) (a) Burling, F. T.; Goldstein, B. M. *Acta Crystallogr.* **1993**, *B49*, 738−744. (b) Szabó, D.; Kuti, M.; Kapovits, I.; Rábai, J.; Kucsman, Á., Argay, G.; Czugler, M.; Kálmán, A.; Párkányi, L. *J. Mol. Struct.* **1997**, *415*, 1−16.
(14) Funabashi, M.; Arai, S.; Shinohara, M. *J. Carbohydr. Chem.* **1999**, *18*, 333−341.
(15) Auzanneau, F. I.; Bundle, R. D. *Carbohydr. Res.* **1991**, *212*, 13−24.
(16) Afonso, C. A. M.; Barros, M. T.; Maycock, C. D. *Tetrahedron* **1999**, *55*, 801−814.
(17) Pozsgay, V.; Jennings, J. H. *J. Org. Chem.* **1988**, *53*, 4042−4052.
(18) Groneberg, R. D.; Miyazaki, T.; Stylianides, N. A.; Schulze, T. J.; Stahl, W.; Schreiner, E. P.; Suzuki. T.; Iwabuchi, Y.; Smith, A. L.; Nicolaou, K. C. *J. Am. Chem. Soc.* **1993**, *115*, 7593−7611.
(19) Cao, S.; Roy, R. *Carbohydr. Lett.* **1996**, *2*, 27−34.

SCHEME 1

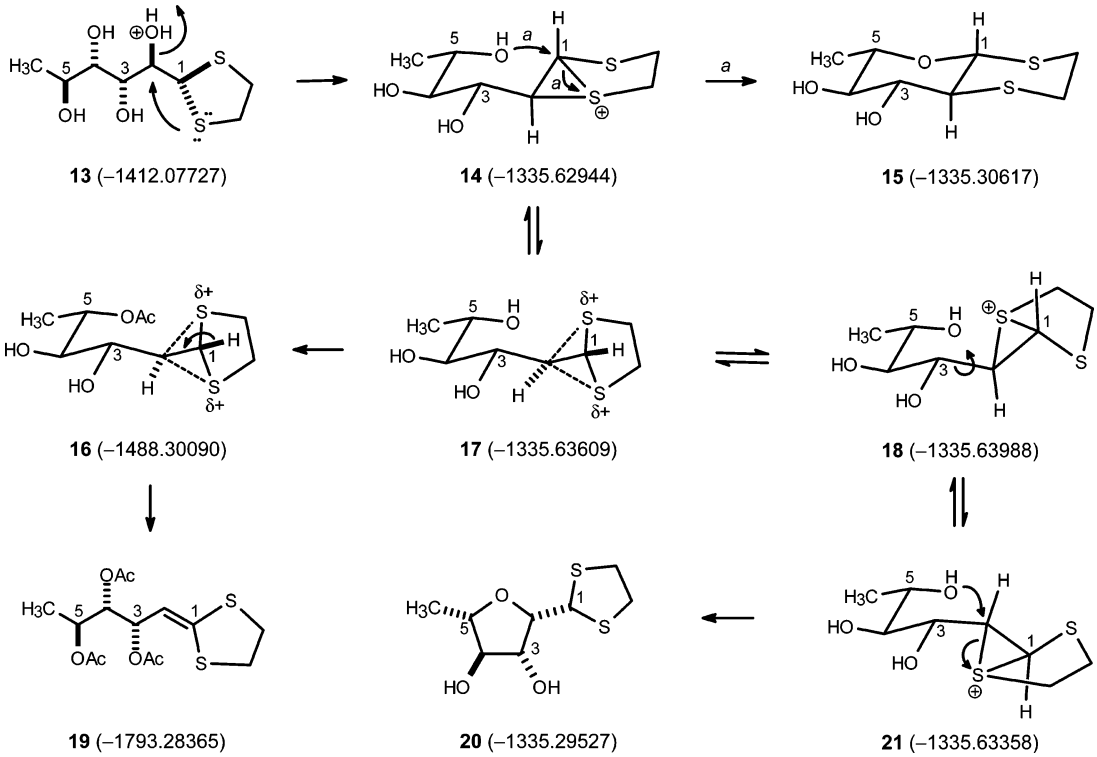

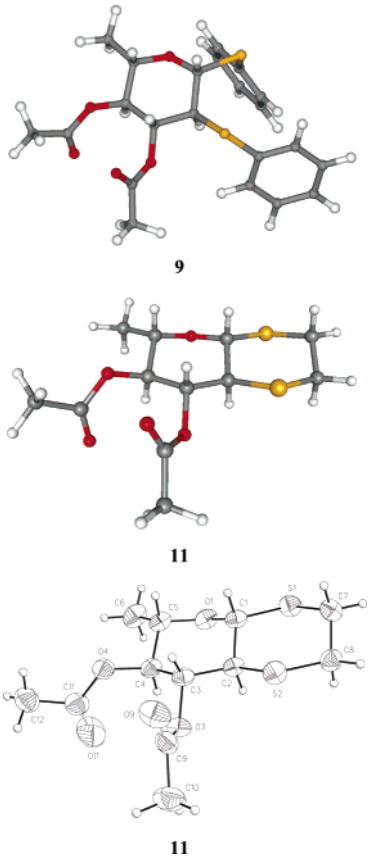

FIGURE 1. Density functional theory (B3LYP/6-31G*) optimized geometry of compounds **9** (top) and **11** (middle) and the X-ray diffraction structure of **11** (bottom).

the range allowed by the constrained geometry of each ring, (b) that the anticlinal geometry could be adjusted for the acetyloxy moieties prior to the minimization procedure but left without restrictions during the calculations, (c) that the conformation of thiophenyl and dithiolanyl moieties could be explored by full rotation of the torsion angles Ph−S−C1−C2 and/or S−C1−C2−C3 in steps of 10°, and (d) that ring inversion of the dithiolanyl fragment would have to be considered for compound **12**. A Monte Carlo protocol[21] was then applied to the structures obtained by the above outlined systematic procedure to explore their complete conformational surface. The global minimum energy conformations were geometrically optimized by DFT (B3LYP/6-31G*) calculations.[22,23] The calculated coupling constants were obtained from the H−C−C−H dihedral angles measured in the minimum energy DFT molecular models by means of the Altona equation.[24,25]

(a) Pyranoside Derivatives 5−9 and 11. The systematic molecular mechanics search, as well as the Monte Carlo protocol for this group of cyclic substances, indi-

(20) (a) Halgren, T. *J. Comput. Chem.* **1996**, *17*, 490−519. (b) Halgren, T. *J. Comput. Chem.* **1996**, *17*, 520−552. (c) Halgren, T. *J. Comput. Chem.* **1996**, *17*, 553−586. (d) Halgren, T.; Nachbar, R. B. *J. Comput. Chem.* **1996**, *17*, 587−615. (e) Halgren, T. *J. Comput. Chem.* **1996**, *17*, 616−641.

(21) Chang, G.; Guida, W. C.; Still, W. C. *J. Am. Chem. Soc.* **1989**, *111*, 4379−4386.

(22) Kong, J.; White, C. A.; Krylov, A. I.; Sherrill, C. D.; Adamson, R. D.; Furlani, T. R.; Lee, M. S.; Lee, A. M.; Gwaltney, S. R.; Adams, T. R.; Ochsenfeld, C.; Gilbert, A. T. B.; Kedziora, G. S.; Rassolov, V. A.; Maurice, D. R.; Nair, N.; Shao, Y.; Besley, N. A.; Maslen, P. E.; Dombroski, J. P.; Daschel, H.; Zhang, W.; Korambath, P. P.; Baker, J.; Byrd, E. F. C.; Van Voorhis, T.; Oumi, M.; Hirata, S.; Hsu, C.-P.; Ishikawa, N.; Florian, J.; Warshel, A.; Johnson, B. G.; Gill, P. M. W.; Head-Gordon, M.; Pople, J. A. *J. Comput. Chem.* **2000**, *21*, 1532−1548.

(23) Hehre, W. J.; Radom, L.; Schleyer, P. V. R.; Pople, J. A. *Ab Initio Molecular Orbital Theory*; Wiley: New York, 1986.

(24) Haasnoot, C. A. G.; de Leeuw, F. A. A. M.; Altona, C. *Tetrahedron* **1980**, *36*, 2783−2792.

(25) Cerda-García-Rojas, C. M.; Zepeda, L. G.; Joseph-Nathan, P. *Tetrahedron Comput. Methodol.* **1990**, *3*, 113−118.

TABLE 1. Density Functional Theory (B3LYP/6-31G*) Total Energy (hartrees), Calculated H−C−C−H Dihedral Angles (deg), and Calculated and Observed[a] ^{1}H−^{1}H Vicinal Coupling Constants (Hz) for the Pyranose Ring of Compounds 5−9 and 11 and Comparison with the X-ray Data of 11

compd	E_{DFT}	$\phi_{H1-C-C-H2}$	$J_{1,2(calcd)}$	$J_{1,2(obsd)}$	$\phi_{H2-C-C-H3}$	$J_{2,3(calcd)}$	$J_{2,3(obsd)}$	$\phi_{H3-C-C-H4}$	$J_{3,4(calcd)}$	$J_{3,4(obsd)}$	$\phi_{H4-C-C-H5}$	$J_{4,5(calcd)}$	$J_{4,5(obsd)}$
5	−1165.959 467	73.8	1.3	1.5	51.3	3.3	3.3	−177.3	9.5	9.3	−178.8	9.2	9.3
6	−1623.957 632	65.8	1.8	1.6	57.0	2.7	3.3	−172.0	9.2	9.8	171.5	9.1	9.8
7	−1165.962 107	−57.2	0.9	1.2	53.2	3.1	3.5	−173.3	9.1	9.2	179.8	9.2	9.2
8	−1623.956 939	−54.6	1.2	1.2	52.8	3.2	3.4	−176.9	9.7	10.1	−178.6	9.3	9.4
9	−2025.312 698	−167.5	10.7	11.0	164.3	10.0	11.0	−164.8	8.1	9.5	176.8	9.3	9.5
11	−1640.639 592	−175.2	10.9	9.5	169.0	10.6	10.5	−163.6	8.0	9.3	173.6	9.2	9.5
11[b]		−179.1	10.8		173.5	10.8		−168.3	8.4		−178.8	9.3	

[a] Measured in $CDCl_3$ solutions. [b] From X-ray diffraction coordinates.

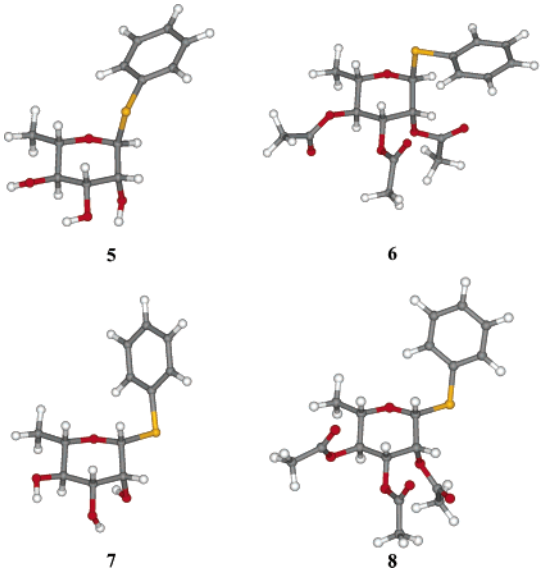

FIGURE 2. Density functional theory molecular models (B3LYP/6-31G*) of pyranoside derivatives **5**−**8**.

cated that the six-membered ring of the pyranoside derivatives mainly exists in a single preferred chair conformation. Table 1 lists the DFT total energy for the most stable conformers of **5**−**9** and **11**, the calculated H−C−C−H dihedral angles of the pyranose rings, and a comparison between the calculated and observed ^{1}H−^{1}H vicinal coupling constants validating the experimental conformation of the six substances. The pyranose ring of compound **5** (Figure 2) exists in a chair conformation moderately distorted (11%) with a H1−C1−C2−H2 dihedral angle of 74°. The chair distortion may be caused by the steric hindrance of the axial orientation of the thiophenyl group as well as by the syn orientation of the phenyl group with an O1−C1−S1−C_{ipso} torsion angle of −77°. The pyranose rings of compounds **6**−**8** are slightly distorted chairs, with distortion percentages of 7%, 9%, and 6%, respectively. It is noteworthy that the minimum energy conformation of thiopyranosides **5**, **7**, and **8** possesses a syn-oriented phenyl group in relation to the pyranoside oxygen atom while in the triacetyl derivatives **6** the phenyl group remains anti-oriented (Figure 2). A detailed description of the pyranose ring conformations was obtained through the use of the polar set of Cremer and Pople[26] parameters (angular variables θ and ϕ as well as the total puckering amplitude Q), which were calculated from the atomic coordinates of the DFT molecular models. These parameters and a description of the six-membered ring conformation of **5**−**9** and **11** are shown in Table 2. According to these summarized results, the pyranose ring of compounds **9** and **11** (Figure 1) exhibited a distorted chair conformation, whereas the dithiane moiety of compound **11** exists in a conformation very close to the classical chair form. For all the calculated pyranoside rings, the chair distortion ranged from 6% to 13%. Consistently, the X-ray structure of **11** showed the pyranoside ring distorted by 11% (Table 2). A comparison between the X-ray diffraction structure and the DFT optimized geometry of the dithiinopyran **11** (Figure 1) shows that the conformation of the two heterocyclic rings is similar in both the solid state and in the calculated molecular model. The RMS value between the X-ray structure of **11** and its DFT molecular model was 0.073 Å for the non-hydrogen atoms of the dithiinopyran moiety and 0.299 Å including the methyl and acetoxyl groups. The X-ray diffraction bond angles and interatomic distances of the 1,4-dithiane ring of **11** are summarized in Table 3 together with the corresponding DFT calculated parameters. Both structural features were in good agreement with the previously reported data for the 1,4-dithiane.[27]

(b) 2,5-Anhydrohexose Derivatives 10 and 12. Application of the Monte Carlo method to structures **10** and **12**, followed by a conformational systematic classification according to their geometrical parameters (essentially Ph−S−C1−C2, O1−C2−C1−S, and C2−C3−C4−C5 dihedral angles) and the molecular mechanics energy (0−5 kcal/mol), revealed the presence of three relevant conformers for the tetrahydrofuran ring as well as three entities produced by the rotation of the C1−C2 bond. The highly flexible dithiophenyl moiety of **10** allowed for a large number of conformational variants, but the selected energy window limited the possibilities to only 15 conformers from the energetically wide conformational dispersion inherent to this structure. Dithiolane **12** possessed fewer degrees of freedom and an energetically narrower conformational divergence affording 16 conformations. A selection of the three most stable conformers from each of the two groups obtained, which represented all the C1−C2 rotameric species, were geometry optimized by using a DFT hybrid at the 6-31G*/B3LYP level of theory.[22,23] The minimun energy conformations are listed in Table 2 and their corresponding energies in Table 4. The pseudorotation of the furanoside

(26) Cremer, D.; Pople, J. A. *J. Am. Chem. Soc.* **1975**, *97*, 1354−1358.

(27) Dávalos, J. Z.; Flores, H.; Jiménez, P.; Notario, R.; Roux, M. V.; Juaristi, E.; Hosmane, R. S.; Liebman, J. F. *J. Org. Chem.* **1999**, *64*, 9328−9336.

TABLE 2. Density Functional Theory (B3LYP/6-31G*) Conformation for the Heterocyclic Rings of 5−12

compd (ring)	conformational contributions[a]			ring conformation	conformational params		
	chair	boat	twist-boat		Q[b]	ϕ[c]	θ[c]
5 (O−C1−C2−C3−C4−C5)[d]	89	5	6	distorted chair	0.55	17.32	7.02
6 (O−C1−C2−C3−C4−C5)[d]	93	2	5	distorted chair	0.55	20.01	4.25
7 (O−C1−C2−C3−C4−C5)[d]	91	8	1	distorted chair	0.59	4.27	5.84
8 (O−C1−C2−C3−C4−C5)[d]	94	6	0	distorted chair	0.58	1.46	3.80
9 (O−C1−C2−C3−C4−C5)[d]	87	5	8	distorted chair	0.55	18.15	8.74
11 (O−C1−C2−C3−C4−C5)[d]	90	8	2	distorted chair	0.57	6.66	6.26
11 (C1−C2−S−C8−C7−S)[d]	98	2	0	chair	0.72	6.23	1.17
11 (O−C1−C2−C3−C4−C5)[e]	89	5	6	distorted chair	0.58	17.37	7.14
11 (C1−C2−S−C8−C7−S)[e]	95	0	5	chair	0.72	29.78	3.79

compd (ring)	conformational contributions[a]		ring conformation	conformational params	
	envelope	twist		Q[b]	ϕ[c]
10A (O−C2−C3−C4−C5)[d]	66	34	^{1}E	0.38	6.12
10P (O−C2−C3−C4−C5)[d]	48	52	^{3}T$_4$	0.37	9.37
10M (O−C2−C3−C4−C5)[d]	79	21	^{5}E	0.35	3.75
12A (O−C2−C3−C4−C5)[d]	32	68	^{1}T$_2$	0.36	12.35
12M (O−C2−C3−C4−C5)[d]	57	43	^{3}T$_4$	0.35	7.70
12P (O−C2−C3−C4−C5)[d]	34	66	^{5}T$_4$	0.37	11.93
12A (C1−S−C7−C8−S)[d]	66	34	between envelope and twist	0.48	6.03
12M (C1−S−C7−C8−S)[d]	47	53	between envelope and twist	0.47	9.61
12P (C1−S−C7−C8−S)[d]	60	40	between envelope and twist	0.51	7.14

[a] Quantitative contributions of basic conformations in percentage. [b] Total puckering amplitude in angstroms. [c] In degrees. [d] From density functional theory coordinates. [e] From X-ray diffraction coordinates.

TABLE 3. X-ray Interatomic Distances (Å), Bond Angles (deg), and Torsion Angles (deg) of the 1,4-Dithiane Ring of 11 and the Corresponding Density Funtional Theory (B3LYP/6-31G*) Calculated Parameters

param	X-ray data	DFT (B3LYP)	param	X-ray data	DFT (B3LYP)
C1−C2	1.525	1.536	C7−C8−S2	111.6	113.5
C1−S1	1.816	1.842	C1−S1−C7	99.9	99.5
C2−S2	1.824	1.847	C2−S2−C8	99.2	99.7
C7−C8	1.523	1.526	S1−C1−C2−S2	65.6	67.6
S1−C7	1.798	1.836	C2−C1−S1−C7	−57.2	−59.4
S2−C8	1.808	1.834	C1−S1−C7−C8	59.2	58.7
C2−C1−S1	114.3	113.7	S1−C7−C8−S2	−70.1	−67.4
C1−C2−S2	112.4	112.3	C7−C8−S2−C2	62.7	59.9
C8−C7−S1	113.3	113.5	C1−C2−S2−C8	−60.6	−59.6

TABLE 4. Calculated ^{1}H−^{1}H Vicinal Coupling Constants for the H1−C1−C2−H2 Fragment of Compounds 10 and 12 Using Molecular Mechanics and the Density Functional Theory[a]

conformer	molecular mechanics (MMFF)					DFT calculations (B3LYP/6-31G*)				
	E_{MM} (kcal/mol)	n[b]	$\phi_{H1-C1-C2-H2}$ (deg)	$J_{1,2}$ (Hz)	$nJ_{1,2}$ (Hz)	E_{DFT} (hartrees)	n[b]	$\phi_{H1-C1-C2-H2}$ (deg)	$J_{1,2}$ (Hz)	$nJ_{1,2}$ (Hz)
10P	65.911	0.0041	67.2	1.05	0.004	−2025.306449	0.1791	79.0	0.53	0.095
10A	62.665	0.9901	−173. 0	10.48	10.376	−2025.306736	0.2429	170.2	10.87	2.640
10M	65.711	0.0058	−52.2	4.50	0.026	−2025.307555	0.5780	−63.1	2.97	1.717
total		1.0000			10.406 (4.0)		1.0000			4.452 (4.0)
12P	43.419	0.4072	66.8	1.10	0.448	−1640.634842	0.2773	70.4	0.87	0.241
12A	43.207	0.5824	−169. 8	10.17	5.923	−1640.635741	0.7189	−174.9	10.60	7.620
12M	45.592	0.0104	−65.6	2.64	0.027	−1640.630798	0.0038	−65.0	2.71	0.010
total		1.0000			6.398 (7.8)		1.0000			7.871 (7.8)

[a] Experimental values are given in parentheses. [b] Molar fraction at 298 K.

ring[28] of the dithiophenyl derivative **10**, through its stabilized conformations ^{1}E, ^{3}T$_4$, and ^{5}E, is far more extreme than the one calculated for the dithiolanyl **12**, whose resulting conformations were ^{1}T$_2$, ^{3}T$_4$, and ^{5}T$_4$. Both sets of movements follow a comparable pathway as reflected by the quantitative Cremer and Pople parameters (Table 2).

The calculated coupling constants of **10** and **12** were estimated by taking into consideration the corresponding molar fraction based on Boltzmann populations in relation to the DFT energy values of each conformer.[10] The experimental vicinal coupling constants for the protons attached to the tetrahydrofuran moiety (H2 through H5) of both derivatives were in agreement when the presence of the three calculated main conformations for the cyclic moiety were taken into consideration. In contrast, particularly in the case of the dithiophenyl derivative **10**, the difference between the observed and calculated $J_{1,2}$ values (calcd, 10.4 Hz, vs obsd, 4.0 Hz) was remarkably large. This inconsistency appeared when using the mo-

(28) Houseknecht, J. B.; McCarren, P. R.; Lowary, T. L.; Hadad, C. M. *J. Am. Chem. Soc.* **2001**, *123*, 8811−8824.

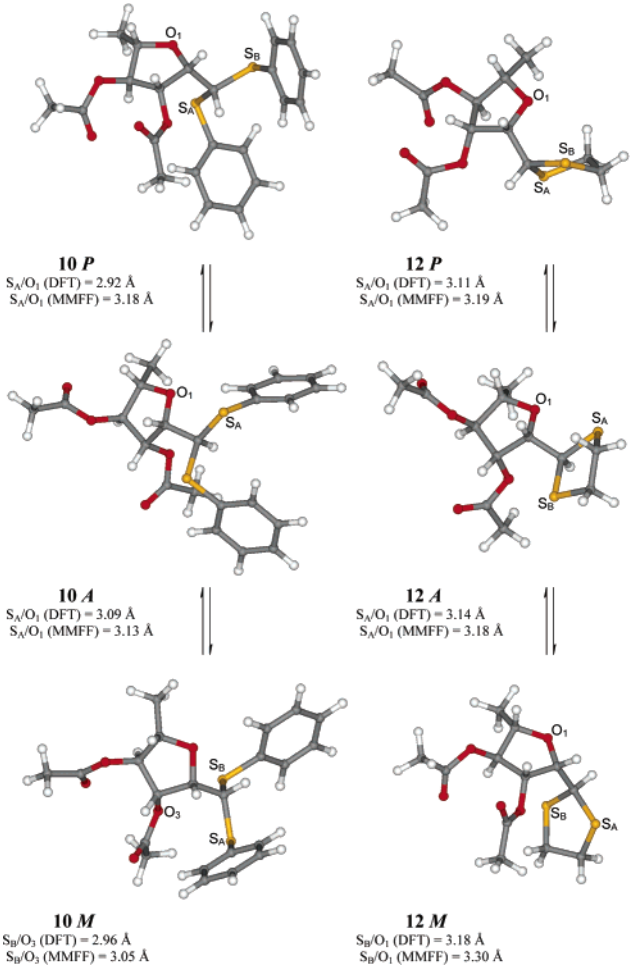

FIGURE 3. Quantum mechanics models (DFT/B3LYP/6-31G*) of 2,5-anhydro-6-deoxyl-L-glucose dithioacetals **10** and **12**.

lecular mechanics approach but was nullified when high levels of quantum mechanics theory were applied. It can be assumed that the large $J_{1,2}$ vicinal coupling constant (Table 4), calculated by MMFF molecular mechanics, indicated that the conformer with H1 and H2 in an anti orientation is the most stable if only steric effects were considered. On the other hand, the notable convergence in the $J_{1,2}$ value, when the DFT calculations were applied, suggested a strong influence of electronic interactions. Figure 3 shows the geometrically optimized minimum energy conformers, and the S···O interatomic distances corresponding to the 1,4 and 1,5 electrostatic sulfur−oxygen intramolecular interactions are included, which in all cases were considerably smaller than those found in the molecular mechanics models. The density functional theory sulfur−oxygen interatomic distances noted in Figure 3 were smaller (2.92−3.18 Å) than the sum of the van der Waals radii of the corresponding atoms (3.25−3.30 Å), fully agreeing with the previously reported theoretical values for such interactions.[12,13] These distances were shorter than the molecular mechanics calculated values. Also, the distortion of the H1−C1−C2−H2 dihedral angles with respect to the molecular mechanics models provided additional support for the strength of this atomic interaction (Table 4).

Evidence of the rotameric equilibrium in dithiophenyl

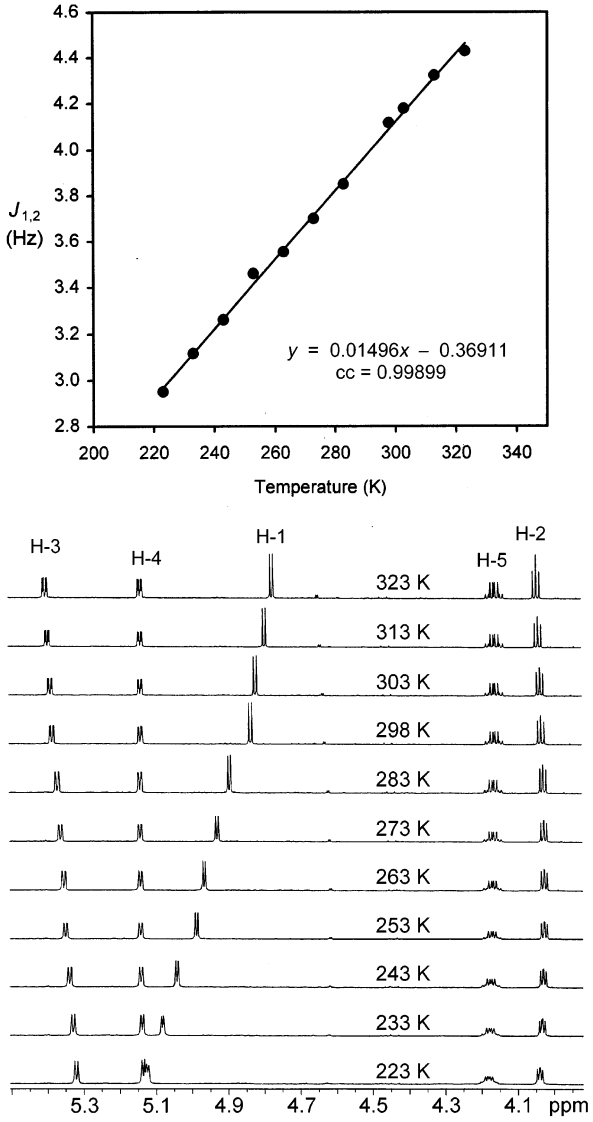

FIGURE 4. ^{1}H NMR spectrum of dithiophenyl derivative **10** as a function of temperature (bottom) and correlation line for the H1−H2 coupling constant temperature dependence variation (top).

derivative **10**, obtained by performing variable-temperature ^{1}H NMR experiments in the range of 223−323 K, supported the S···O electrostatic interactions (Figure 4). Decreasing the temperature favored the stabilization of conformations *minus* and *plus* (**10***M* and **10***P*; Table 4) where the attractive interactions were present. Heating increased the entropy term, resulting in a more evenly rotamerically distributed population. Figure 4 shows that raising the temperature increases the $J_{1,2}$ coupling constant value in agreement with the above-mentioned hypothesis in that the observed coupling constant at 223 K had a value of 2.9 Hz, while at 323 K this value went up to 4.4 Hz. DFT molecular models of derivative **10** were found to overwhelmingly prefer a gauche conformation in which the angle for the segment H1−C1−C2−H2 is distorted by more than 12° when compared to the molecular mechanics models (Figure 3). This situation was quite evidently due to the stabilization gained by the electrostatic attraction between the two involved het-

eroatoms. Averaging the population of the three rotameric species would result in a value of ca. 7 Hz.

Mechanism Involving 1,2-Sulfur Migration in the α-Hydroxyalkyldithioacetal Derivatives. A conceivable mechanistic pathway for the transformation of **3** into **11**, **12**, and **19** is illustrated in Scheme 1. The acidic condition of the acylating agent provoked the nucleophilic attack of the anti-oriented sulfur atom to position C2 in **13** (Scheme 1), resulting in the substitution of the protonated hydroxyl group. The nuclephilic action of the C5 oxygen atom on C1 could cause a molecular rearrangement in the generated thiiranium ion (**14**) with a consequent C−S bond breakage to yield dithiinopyran **15**. A similarly described 1,2-sulfur migration, with the participation of a three-membered ring sulfonium ion intermediate,[15] occurred in α-hydroxyalkyldithioacetals.[16] On the other hand, the sulfonium ion **14** could also reach an equilibrium with **18** through intermediate **17**, and the C2−C3 bond rotation of **18** could lead to **21**. The hydroxyl group located at C-5 in **21** attacked position C2 and yielded 2,5-anhydro-L-rhamnose ethylenedithioacetal (**20**). The resulting five-membered ring closure was possible because conformation **21** possessed the adequate spatial orientation. However, if the hydroxyl group at C5 became acetylated, the cyclization reaction would be prevented. In which case intermediate **16** could be stabilized by the loss of a proton from C1, resulting in an unsaturated substance whose complete acetylation yielded alkene **19**. Similarly, intermediates **15** and **20** must undergo a full acetylation to yield **11** and **12**. The tridimensional structures of all above-mentioned intermediates (Scheme 1) were calculated at the DFT (B3LYP/6-31G*) level of theory, allowing a clear visualization of the 1,2-sulfur migrations supported by the reaction energetics. DFT energy values (hartrees) were also included for each intermediate. This theoretical approach also helped us to explain the formation of the unexpected rearranged products through the postulation of feasible intermediates. Compounds **11**, **12**, and **19** were obtained in 40%, 1.6%, and 0.5% yields, respectively. Intermediate **15** affords **11** and is by far more stable (6.84 kcal/mol) than intermediate **20**, which in turn yields **12**. However, the presence of **12** and **19** as reaction products may be attributed to the higher stability of intermediates **17**, **18**, and **21** over intermediate **14**.

Conclusions

The present study represents an example of how the application of quantum mechanics calculations can be used to understand the conformational behavior of sulfur-containing monosaccharide derivatives. This approach also lends itself to the exploration of the relevance of the electrostatic intramolecular attraction between sulfur and oxygen (which might also operate in complex biomolecules[6]) with its implication in reaction mechanisms. Through the above-described energetical and geometrical evidence, the conformation of compounds **10** and **12** reflects the dominance of electrostatic sulfur−oxygen intramolecular attractions over steric effects. The synthesis and conformational analysis by molecular modeling and NMR spectroscopy of sulfur-containing 6-deoxy-L-hexose derivatives, used as enantiopure building blocks for the acyclic moiety of cytotoxic polyoxygenated 6-heptenyl-5,6-dihydro-α-pyrones, will be the subject of further investigations in our laboratories.

Experimental Section

Treatment of 6-Deoxy-L-mannose with Benzenethiol. A mixture of 6-deoxy-L-mannose (500 mg, 2.74 mmol) and benzenethiol (1.5 mL, 14.6 mmol) in 90% trifluoroacetic acid was stirred at 55 °C for 1 h. The reaction mixture was evaporated to dryness under an Ar flow, and the residue was purified by column chromatography on Si gel (100 g). Elution with 19:1 CH_2Cl_2/MeOH afforded derivative **1** (515 mg, 51%, $R_f = 0.43$) and a mixture of **5** and **7** (235 mg, 36%, $R_f = 0.36$, 9:1 CH_2Cl_2/MeOH). This mixture was submitted to normal-phase preparative HPLC using an isocratic elution with CH_2Cl_2/MeOH (49:1) and a flow rate of 6 mL/min to yield compounds **5** (33 mg, 4%, $t_R = 17.1$ min) and **7** (58 mg, 8%, $t_R = 19.3$ min).

Phenyl 1-Thio-6-deoxy-α-L-mannopyranoside (5): white solid; mp 86−88 °C (lit.[18] mp 99 °C); ORD (*c* 0.19, MeOH) $[\alpha]_{589}$ −233, $[\alpha]_{578}$ −243, $[\alpha]_{546}$ −278, $[\alpha]_{436}$ −493, $[\alpha]_{365}$ −843; ^{1}H NMR (500 MHz, C_5D_5N) δ 7.66−7.64, 7.30−7.18, 6.08 (dd, $J = 1.4$, 0.5 Hz, H1), 4.76 (dd, $J = 3.3$, 1.5 Hz, H2), 4.62 (dq, $J = 9.3$, 6.2, H5), 4.44 (dd, $J = 9.3$, 3.3, H3), 4.32 (dd, $J = 9.3$, 9.3, H4), 1.61 (d, $J = 6.2$, H6); ^{13}C NMR (125.7 MHz, C_5D_5N) δ 136.1, 131.4 (×2), 129.4 (×2), 127.2, 90.0 (C1), 74.0 (C4), 73.8 (C2), 73.3 (C3), 71.2 (C5), 18.4 (C6); EIMS (20 eV) *m*/*z* (rel intens) $[M]^+$ 256 (25), $[M - C_6H_5S]^+$ 147 (100), 146 (13), $[147 - H_2O]^+$ 129 (68), 111 (17), $[C_6H_6S]^+$ 110 (60), $[C_6H_5S]^+$ 109 (16), 87 (15), $[129 - C_2H_4O]^+$ 85 (95), 83 (14), 75 (17), 73 (24), $[85 - CH_2]^+$ 71 (93), 61 (27), 60 (10), 59 (40), 58 (10), 57 (40), 55 (18), 45 (23), 43 (37), 41 (20), 31 (9), 29 (14); HREIMS (70 eV) *m*/*z* $[M]^+$ 256.0774 (calcd for $C_{12}H_{16}O_4S$ 256.0769).

Phenyl 1-Thio-6-deoxy-β-L-mannopyranoside (7): white solid; mp 142−144 °C; ORD (*c* 0.71, MeOH) $[\alpha]_{589}$ +70, $[\alpha]_{578}$ +73, $[\alpha]_{546}$ +83, $[\alpha]_{436}$ +147, $[\alpha]_{365}$ +245; ^{1}H NMR (500 MHz, C_5D_5N) δ 7.74−7.71, 7.65−7.63, 7.36−7.20, 5.35 (d, $J = 1.2$ Hz, H1), 4.64 (dd, $J = 3.5$, 1.2 Hz, H2), 4.17 (dd, $J = 9.2$, 9.2 Hz, H4), 4.09 (dd, $J = 9.2$, 3.5 Hz, H3), 3.72 (dq, $J = 9.2$, 6.1 Hz, H5), 1.58 (d, $J = 6.1$ Hz, H6); ^{13}C NMR (125.7 MHz, C_5D_5N) δ 137.6, 129.7 (×2), 129.2 (×2), 126.5, 88.3 (C1), 77.5 (C5), 76.1 (C3), 74.0 (C2), 73.3 (C4), 18.6 (C6); EIMS (20 eV) *m*/*z* (rel intens) $[M]^+$ 256 (8), $[M - C_6H_5S]^+$ 147 (64), $[147 - H_2O]^+$ 129 (50), 111 (15), $[C_6H_6S]^+$ 110 (47), $[C_6H_5S]^+$ 109 (12), 87 (14), $[129 - C_2H_4O]^+$ 85 (96), $[85 - CH_2]^+$ 71 (100), 59 (43), 58 (11), 57 (47), 55 (20), 45 (28), 43 (45), 41 (26), 31 (12), 29 (17); HREIMS (70 eV) *m*/*z* $[M]^+$ 256.0774 (calcd for $C_{12}H_{16}O_4S$ 256.0769).

General Procedure for Acetylation. A solution of the starting material (1 mmol) in acetyl chloride (100 mmol), used as provided by the manufacturer without purification, was stirred at room temperature for 2 h and evaporated under a N_2 flow. Column chromatography on Si gel (1:100) with a gradient of EtOAc in *n*-hexane afforded the corresponding peracetyl derivative.

Phenyl 2,3,4-Tri-*O*-acetyl-1-thio-6-deoxy-α-L-mannopyranoside (6). Acetylation of **5** (54 mg) yielded **6** (45.2 mg, 67%, $R_f = 0.42$, 7:3 *n*-hexanes/EtOAc): white solid; mp 114−116 °C (lit.[17] mp 116−118 °C); ORD (*c* 9.71, $CHCl_3$) $[\alpha]_{589}$ −90, $[\alpha]_{578}$ −94, $[\alpha]_{546}$ −107, $[\alpha]_{436}$ −185, $[\alpha]_{365}$ −297; EIMS (20 eV) *m*/*z* (rel intens) $[M]^+$ 382 (0.1), 275 (2), 274 (9), $[M - C_6H_5S]^+$ 273 (67), $[273 - C_2H_4O_2]^+$ 213 (20), $[213 - C_2H_2O]^+$ 171 (27), 154 (9), $[171 - H_2O]^+$ 153 (100), 129 (10), $[171 - C_2H_4O_2]^+$ 111 (92), $[111 - CO]^+$ 83 (31), $[C_2H_3O]^+$ 43 (59); positive FAB-MS *m*/*z* (rel intens) $[M + Na]^+$ 405 (10), $[M + H]^+$ 383 (7), $[M]^+$ 382 (4), $[M + H - C_2H_4O_2]^+$ 323 (6), $[M + H - SC_6H_5]^+$ 273 (100), 213 (20), 203 (27), 171 (21), 154 (28), 153 (64), 137 (12), 136 (24), 111 (64), 83 (27), 43 (63).

Phenyl 2,3,4-Tri-*O*-acetyl-1-thio-6-deoxy-β-L-mannopyranoside (8). Acetylation of **7** (81 mg) yielded **8** (64.5 mg, 53%, $R_f = 0.35$, 7:3 *n*-hexanes/EtOAc): oil;[19] ORD (*c* 6.35, $CHCl_3$) $[\alpha]_{589}$ +36, $[\alpha]_{578}$ +37, $[\alpha]_{546}$ +42, $[\alpha]_{436}$ +72, $[\alpha]_{365}$ +110; EIMS

(20 eV) *m/z* (rel intens) $[M]^+$ 382 (0.27), $[M - C_6H_5S]^+$ 273 (65), $[273 - C_2H_4O_2]^+$ 213 (17), $[213 - C_2H_2O]^+$ 171 (27), $[171 - H_2O]^+$ 153 (100), $[171 - C_2H_4O_2]^+$ 111 (84), $[111 - CO]^+$ 83 (44), $[C_2H_3O]^+$ 43 (88); positive FAB-MS *m/z* (rel intens) $[M + Na]^+$ 405 (3), $[M + H]^+$ 383 (13), $[M]^+$ 382 (5), 289 (12), 275 (12), 274 (67), $[M + H - SC_6H_5]^+$ 273 (100), 231 (12), 221 (12), 213 (32), 204 (20), 203 (10), 189 (16), 171 (30), 154 (33), 153 (63), 138 (15), 137 (20), 136 (30), 129 (10), 111 (62), 107 (10), 83 (24), 43 (79).

Treatment of 6-Deoxy-L-mannose Diphenyldithioacetal with Acetyl Chloride. Acetylation of **1** (440 mg) yielded compound **2** (206.4 mg, 32.2%, $R_f = 0.46$), compound **9** (67 mg, 12.9%, $R_f = 0.53$), and compound **10** (23.9 mg, 4.6%, $R_f = 0.49$, 7:3 *n*-hexane/EtOAc).

Phenyl 3,4-Di-*O*-acetyl-2-S-phenyl-1,2-dithio-6-deoxy-β-L-glucopyranoside (9): white solid; mp 97−99 °C; ORD (*c* 3.67, $CHCl_3$) $[\alpha]_{589}$ +6, $[\alpha]_{578}$ +6, $[\alpha]_{546}$ +8, $[\alpha]_{436}$ +17, $[\alpha]_{365}$ +36; ^{1}H NMR (500 MHz, $CDCl_3$) δ 7.53−7.51, 7.48−7.45, 7.29−7.26, 5.16 (dd, $J = 11.0$, 9.5 Hz, H3), 4.70 (dd, $J = 9.5$, 9.5 Hz, H4), 4.45 (d, $J = 11.0$ Hz, H1), 3.43 (dq, $J = 9.5$, 6.0 Hz, H5), 3.05 (dd, $J = 11.0$, 11.0 Hz, H2), 2.01 (s, 3H), 1.94 (s, 3H), 1.19 (d, $J = 6.0$ Hz, H1); ^{13}C NMR (125.7 MHz, $CDCl_3$) δ 170.1, 169.9, 134.2 (×2), 133.3 (×2), 131.7, 131.5, 129.0 (×2), 128.8 (×2), 128.3, 128.0, 86.3 (C1), 74.5 (C4), 74.2 (C3), 73.8 (C5), 52.3 (C2), 20.7, 20.6, 17.5 (C6); EIMS (20 eV) *m/z* (rel intens) $[M]^+$ 432 (1.1), $[M - C_6H_5S]^+$ 323 (1), $[323 - C_2H_4O_2]^+$ 263 (9), 204 (15), $[263 - C_2H_4O_2]^+$ 203 (100), 177 (4), 149 (4), 139 (7), 137 (5), 111 (8), 110 (7), 97 (5), 83 (14), 71 (6), 69 (7), 57 (8), 44 (6), $[C_2H_3O]^+$ 43 (31); positive FAB-MS *m/z* (rel intens) $[M + Na]^+$ 455 (4), $[M + H]^+$ 433 (4), $[M]^+$ 432 (11), $[M - SC_6H_5]^+$ 323 (37), 307 (30), 289 (22), $[323 - C_2H_4O_2]^+$ 263 (22), 204 (22), $[263 - C_2H_4O_2]^+$ 203 (100), 155 (13), 154 (53), 138 (16), 137 (34), 136 (39), 107 (10), 89 (11), 77 (11), 43 (21). Anal. Calcd for $C_{22}H_{22}O_5S_2$: C, 61.09; H, 5.59; S, 14.82. Found: C,61.06; H, 5.47; S, 14.78.

3,4-Di-*O*-acetyl-2,5-anhydro-6-deoxy-L-glucose Diphenyldithioacetal (10): oil; ORD (*c* 2.41, $CHCl_3$) $[\alpha]_{589}$ +7, $[\alpha]_{578}$ +8, $[\alpha]_{546}$ +9, $[\alpha]_{436}$ +24, $[\alpha]_{365}$ +55; ^{1}H NMR δ (500 MHz, $CDCl_3$) δ 7.51−7.48, 7.38−7.35, 7.31−7.22, 5.39 (dd, $J = 4.5$,1.1 Hz, H3), 5.14 (dd, $J = 4.0$, 1.0 Hz, H4), 4.84 (d, $J = 4.0$ Hz, H1), 4.16 (dq, $J = 6.5$, 4.0 Hz, H5), 4.03 (dd, $J = 4.5$, 4.0 Hz, H2), 2.11 (s, 3H), 2.05 (s, 3H), 1.25 (d, $J = 6.5$ Hz, H6); ^{13}C NMR (125.7 MHz, $CDCl_3$) δ 170.2, 170.0, 134.3, 134.2, 132.9 (×2), 132.7 (×2), 129.0 (×2), 128.9 (×2), 127.9, 127.8, 85.1 (C2), 80.8 (C3), 78.8 (C4), 77.4 (C5), 60.8 (C1), 20.8 (×2), 13.6 (C6); EIMS (20 eV) *m/z* (rel intens) $[M]^+$ 432 (5), $[M - C_6H_5S]^+$ 323 (10), 264 (18), $[323 - C_2H_4O_2]^+$ 263 (100), 221 (34), $[263 - C_2H_4O_2]^+$ 203 (14), 153 (14), 123 (16), 111 (37), 69 (19), $[C_2H_3O]^+$ 43 (55); positive FAB-MS *m/z* (rel intens) $[M + Na]^+$ 455 (1), $[M + H]^+$ 433 (11), $[M]^+$ 432 (14), $[M - SC_6H_5]^+$ 323 (21), $[323 - C_2H_4O_2]^+$ 263 (100), 221 (18), $[263 - C_2H_4O_2]^+$ 203 (23), 154 (16), 111 (15), 43 (11); HREIMS (70 eV) *m/z* $[M]^+$ 432.1060 (calcd for $C_{22}H_{24}O_5S_2$ 432.1065).

Treatment of 6-Deoxy-L-mannose with 1,2-Ethanedithiol. A solution of 6-deoxy-L-mannose (5 g, 27.5 mmol) in acetic acid (50 mL) was treated with boron trifluoride etherate (2 mL) and 1,2-ethanedithiol (12.5 mL) and stirred for 1 h. The reaction mixture was left overnight at room temperature. The product was filtered and washed with chloroform to afford 6-deoxy-L-rhamnose ethylenedithioacetal (**3**) (476 mg, 38%).

Treatment of 6-Deoxy-L-mannose Ethylenedithioacetal with Acetyl Chloride. The general procedure for acetylation was applied to **3** (2.5 g), yielding compound **4** (2.4 g, 56%, $R_f = 0.27$), compound **11** (1.3 g, 40%, $R_f = 0.37$), and a mixture of compounds **12** and **19** (128 mg, $R_f = 0.30$, 7:3 *n*-hexane/EtOAc), which was purified by reversed-phase HPLC with 3:2 MeOH/H_2O at a flow rate of 3.5 mL/min to obtain compounds **12** (48 mg, 1.6%, $t_R = 13.6$ min) and **19** (18 mg, 0.5%, $t_R = 15.8$ min) separately.

(4a*R*,6*S*,7*S*,8*R*,8a*S*)-7,8-Diacetyloxy-6-methylhexahydro-4aH-[1,4]dithiino[2,3b]pyran (11): white prisms; mp 110−112 °C; ORD (*c* 3.58, $CHCl_3$) $[\alpha]_{589}$ −14, $[\alpha]_{578}$ −15, $[\alpha]_{546}$ −16, $[\alpha]_{436}$ −24, $[\alpha]_{365}$ −29; ^{1}H NMR (500 MHz, $CDCl_3$), δ 4.93 (dd, $J = 10.5$, 9.5 Hz, H3), 4.87 (dd, $J = 9.5$, 9.5 Hz, H4), 3.20 (dd, $J = 10.5$, 9.5 Hz, H2), 3.66 (dq, $J = 9.5$, 6.5 Hz, H5), 4.61 (d, $J = 9.5$ Hz, H1), 3.22 (ddd, $J = 14.0$, 11.5, 2.5 Hz, H7β), 2.99 (ddd, $J = 14.0$, 4.0, 2.5 Hz, H7α), 2.89 (ddd, $J = 14.0$, 11.5, 2.5 Hz, H8α), 2.76 (ddd, $J = 14.0$, 4.0, 2.5 Hz, H8β), 2.06 (s, 3H), 2.03 (s, 3H), 1.24 (d, $J = 6.5$ Hz, H6); ^{13}C NMR (125.7 MHz, $CDCl_3$) δ 170.3, 169.7, 79.1 (C1), 75.2 (C5), 74.4 (C4), 72.3 (C3), 49.6 (C2), 33.1, 29.9, 20.6, 20.5, 17.6 (C6); EIMS (20 eV) *m/z* (rel intens) $[M]^+$ 306 (6), $[M - C_2H_4O_2]^+$ 246 (6), $[246 - C_2H_4O_2]^+$ 186 (34), $[186 - CH_3]^+$ 171 (33), 160 (12), 158 (47), 130 (9), 111 (9), $[C_2H_4S_2]^+$ 92 (100), $[C_2H_3O]^+$ 43 (53); HREIMS (70 eV) *m/z* $[M]^+$ 306.0595 (calcd for $C_{12}H_{18}O_5S_2$ 306.0596).

X-ray Analysis of 11. Single crystals of **11** were grown by slow crystallization from CH_2Cl_2/hexane. They were orthorhombic, space group $P2_12_12_1$, with $a = 9.1347(3)$ Å, $b = 9.4741(3)$ Å, $c = 18.1026(6)$ Å, cell volume 1566.65(9) Å^3, $\rho_{calcd} = 1.30$ g/cm^3 for $Z = 4$, MW = 306.38, and $F(000)e^- = 648$. The intensity data were measured on a Bruker AXS Smart 6000 CCD diffractometer equipped with Mo Kα radiation ($\lambda = 0.71073$ Å). The size of the crystal used was 0.47 × 0.33 × 0.38 mm^3. A total of 10469 reflections were collected at 293 K within a θ range of 2.25−26.00°. They were corrected for background, Lorentz polarization, and absorption ($\mu = 0.351$ mm^{-1}) effects, while crystal decay was negligible. The number of independent reflections was 3086 with $R_{int} = 3.9\%$, and the number of observed reflections was 2659 [$I > 2\sigma(I)$]. The structure was solved by direct methods using SHELXS97.[29] For the structural refinement the non-hydrogen atoms were treated anisotropically, and the hydrogen atoms, included in the structure factor calculation, were refined isotropically. Final discrepancy indices were $R_F = 4.2\%$ and $R_W = 9.6\%$ using a unit weight for the 2659 reflections and refining 193 parameters. The final difference Fourier map was essentially featureless, the highest residual peaks having densities of 0.22 e/A^3. Crystallographic data for **11** have been deposited with the Cambridge Crystallographic Data Centre as Supplementary Publication Number CCDC 213485. Copies of the data can be obtained, free of charge, on application to the Director, CCDC, 12 Union Rd., Cambridge CB2 1EZ, U.K. Fax: +44-(0)1223-336033. E-mail: deposit@ccdc.cam.ac.uk.

3,4-Di-*O*-acetyl-2,5-anhydro-6-deoxy-L-glucose Ethylenedithioacetal (12): oil, ORD (*c* 5.2, $CHCl_3$) $[\alpha]_{589}$ +6, $[\alpha]_{578}$ +6, $[\alpha]_{546}$ +7, $[\alpha]_{436}$ +11, $[\alpha]_{365}$ +15; ^{1}H NMR (300 MHz, $CDCl_3$), δ 5.14 (dd, $J = 3.9$, 1.2 Hz, H3), 5.12 (dd, $J = 3.9$, 1.2 Hz, H4), 4.65 (d, $J = 7.8$ Hz, H1), 4.21 (dq, $J = 6.3$, 3.9 Hz, H5), 3.86 (dd, $J = 7.8$, 3.9 Hz, H2), 3.31−3.17 (m, 4H), 2.13 (s, 3H), 2.10 (s, 3H), 1.2 (d, $J = 6.3$ Hz, H6); ^{13}C NMR (75.4 MHz, $CDCl_3$) δ 169.9, 169.5, 86.4 (C2), 80.2 (C3), 78.7 (C4), 77.6 (C5), 54.3 (C1), 38.8, 38.4, 21.1, 20.8, 14.0 (C6); EIMS (20 eV) *m/z* (rel intens) $[M]^+$ 306 (5), $[M - C_2H_4O_2]^+$ 246 (17), 202 (5), $[M - C_3H_5S_2]^+$ 201 (53), 186 (6), 141 (23), 107 (10), 106 (6), $[C_3H_5S_2]^+$ 105 (100), 99 (68), 43 (31); HREIMS (70 eV) *m/z* $[M]^+$ 306.0590 (calcd for $C_{12}H_{18}O_5S_2$ 306.0596).

3,4,5-Tri-*O*-acetyl-1-anhydro-2,6-dideoxy-L-mannose Ethylenedithioacetal (19): oil, ORD (*c* 0.35, $CHCl_3$) $[\alpha]_{589}$ +29, $[\alpha]_{578}$ +31, $[\alpha]_{546}$ +37, $[\alpha]_{436}$ +89, $[\alpha]_{365}$ +214; ^{1}H NMR (300 MHz, $CDCl_3$) δ 6.3 (s, H2), 5.38 (dd, $J = 5.9$, 5.4 Hz, H4), 5.30 (d, $J = 5.4$ Hz, H3), 5.06 (dq, $J = 6.3$, 5.9 Hz, H5), 3.23−3.03 (m, 4H), 2.11 (s, 3H), 2.07 (s, 3H), 1.24 (d, $J = 6.3$ Hz, H6); ^{13}C NMR (75.4 MHz, $CDCl_3$) δ 170.0, 169.8, 169.5, 122.8 (C1), 116.3 (C2), 74.3 (C3), 73.2 (C4), 67.7 (C5), 27.4, 26.5, 21.1, 20.8 (×2), 15.6 (C6); EIMS (20 eV) *m/z* (rel intens) $[M]^+$ 348 (10.5), $[M - C_2H_4O_2]^+$ 288 (9), $[288 - C_2H_2O]^+$ 246 (6), 203 (9), 189 (13), 188 (10), 187 (16), 186 (100), 185 (5), 160 (7), 159 (6), 158 (7), 153 (5), 149 (9), 148 (8), 147 (96), 146 (10), 145 (7), 126 (9), 117 (8), 43 (33); HREIMS (70 ev) *m/z* $[M]^+$ 348.0705 (calcd for $C_{14}H_{20}O_6S_2$ 348.0701).

(29) Sheldrick, G. M. *Programs for Crystal Structure Analysis*; Institüt für Anorganische Chemie der Universität, University of Göttingen: Göttingen, Germany, 1998.

Molecular Modeling Calculations. Geometry optimizations were carried out using the MMFF94 force-field calculations[20] as implemented in the Spartan'02 molecular modeling software from Wavefunction, Inc. (Irvine, CA). The systematic conformational searches for the five- and six-membered rings were carried out with the aid of Dreiding models considering torsion angle movements of ca. 30°. The E_{MMFF} values were used as the convergence criterion, and a further search with the Monte Carlo protocol[21] was carried out considering an energy cutoff of 5 kcal/mol above the global minimum. Within this range, sets of 15, 38, 4, 16, 28, 15, 8, and 16 different conformations were found and geometry analyzed for **5**−**12**, respectively. The molecular mechanics global minima of **5**−**9** and **11** and the three more stable rotameric species of **10** and **12** were submitted to density functional theory calculations (DFT/B3LYP/6-31G*).[22,23] Conversions from dihedral angles to vicinal coupling constants ($^3J_{HH}$) for each conformer were done using the Altona equation.[24,25] The population-weighted average coupling constant for each H−C−C−H dihedral fragment was calculated using the equation $^3J_{calcd} = n_1J_1 + n_2J_2 + \sum n_iJ_i$. For compounds **10** and **12** a cyclic equilibrium at 298 K between the three selected conformers included in Table 4 was assumed, which afforded $k_{1,2} = n_2/n_1$, $k_{2,3} = n_3/n_2$, $k_{3,1} = n_1/n_3$, and $n_1 + n_2 + n_3 = 1$.[10,30] Taking into account the Boltzmann equation $n_i = e^{-\Delta Ei/kT}/\sum_j e^{-\Delta Ej/kT}$, where ΔE is the DFT energy difference between pairs of conformers, equations $n_1 = n_2e^{-(E2-E1/kT)}$ and $n_3 = n_2e^{-(E2-E3/kT)}$ were then solved to calculate the molar fraction of each conformer.

(30) Arnó, M.; Marín, M. L.; Zaragozá, R. J. *Magn. Reson. Chem.* **1998**, *36*, 579−586.

Acknowledgment. This research was supported by grants from the Consejo Nacional de Ciencia y Tecnología (CONACyT; 32031-N and 39951-Q) and Dirección General de Asuntos del Personal Académico, Universidad Nacional Autónoma de México (UNAM; IN200902-2). M.F.-S. acknowledges a postdoctoral fellowship from CONACyT (Grant 2378). We thank Dr. J. Martín Torres Valencia (Universidad Autónoma del Estado de Hidalgo) for providing the raw X-ray data. Also, thanks are due to the "Unidad de Servicios de Apoyo a la Investigación" (Facultad de Química, UNAM), especially to Marisela Gutiérrez, Oscar Yáñez, and Georgina Duarte for the recording of IR, NMR, and MS spectra, as well as to Margarita Guzmán for the elemental analyses. We are deeply indebted to Ms. Helen Bickham for style corrections.

Supporting Information Available: ^1H and ^{13}C NMR spectra of compounds **5**−**12** (Figures S1−S16), DFT (B3LYP/6-31G*) Cartesian coordinates of minimum energy structures of **5**−**9** and **11** (Tables S1−S5 and S-9), DFT (B3LYP/6-31G*) Cartesian coordinates of **10** and **12** rotamers (Tables S6−S8 and S10−S12), and X-ray crystallographic data of **11** (Tables S13−S18). This material is available free of charge via the Internet at http://pubs.acs.org.

JO034492K